

Review

# N,O-Type Carborane-Based Materials

José Giner Planas \*, Francesc Teixidor and Clara Viñas

Institut de Ciència de Materials de Barcelona (ICMAB-CSIC), Campus U.A.B., 08193 Bellaterra, Spain; teixidor@icmab.es (F.T.); clara@icmab.es (C.V.)

\* Correspondence: jginerplanas@icmab.es; Tel.: +34-093-580-1853

Academic Editor: Umit B. Demirci

Received: 29 March 2016; Accepted: 27 April 2016; Published: 4 May 2016

**Abstract:** This review summarizes the synthesis and coordination chemistry of a series of carboranyl ligands containing N,O donors. Such carborane-based ligands are scarcely reported in the literature when compared to other heteroatom-containing donors. The synthetic routes for metal complexes of these N,O-type carborane ligands are summarized and the properties of such complexes are described in detail. Particular attention is paid to the effect that the incorporation of carboranes has into the coordination chemistry of the otherwise carbon-based ligands and the properties of such materials. The reported complexes show a variety of properties such as those used in magnetic, chiroptical, nonlinear optical, catalytic and biomedical applications.

**Keywords:** metal complexes; carboranes; functional materials; N,O-donors; reactivity; chirality

## 1. Introduction

The icosahedral *closo* carboranes (dicarba-*closo*-dodecaboranes;  $C_2B_{10}H_{12}$ ) are an interesting class of exceptionally stable boron-rich clusters with high thermal and chemical stability, hydrophobicity and acceptor character [1–3]. Carborane chemistry has experienced a major surge of interest across a wide spectrum of technologies, fueled by developing applications in diverse areas such as in catalysis, materials science and medicine [1,4–11]. There are three isomers of carborane that differ in the relative position of both carbon atoms in the clusters (*ortho*-, *meta*- and *para*-, or *o*-, *m*- and *p*-; Figure 1). Although the volume of the three isomers of carborane is roughly the same, they show very different dipole moments as a consequence of the different arrangement of the carbon atoms in the cluster (4.53 D, 2.85 D and zero D for *o*-, *m*- and *p*-, respectively) [8]. The average size of the three isomers of carborane (141–148 Å<sup>3</sup>) is comparable to that of adamantane (136 Å<sup>3</sup>), significantly larger (40%) than the phenyl ring rotation envelope (102 Å<sup>3</sup>) and slightly smaller (10%) than C<sub>60</sub> (160 Å<sup>3</sup>) [12]. The presence of ten hydridic hydrogens at the boron atoms of the clusters makes them extremely hydrophobic, surpassing that for adamantane [13]. The hydrophobicity of carboranes has been extensively used to trigger desired biological actions [7,8]. Concerning the electronic effect, all cluster carbon atoms exert an electron-withdrawing effect on attached substituents, which decreases in the order *o*- to *m*- to *p*-carborane. For example, when bonded by a cluster carbon atom, *o*-carborane exhibits an electron-withdrawing substituent effect similar to that of a fluorinated aryl group. Experimental evidence shows that the electron-withdrawing character of the carborane isomers has a clear impact on the acidity of substituents at carbon, the acidity decreasing in the same order (*o*-, *m*-, *p*-), and all being more acidic than the related phenyl moiety [3]. Thus, the C–H bonds of the icosahedral *closo* carboranes can be deprotonated with strong bases (e.g., alkyllithium) and the generated carboranyl nucleophile can react with a wide variety of electrophiles (e.g., alkylhalides, carbonyl derivatives, etc.) producing C–functionalized carboranes. Monosubstitution of the carboranes is not trivial because the monolithiation of the *o*-carborane moiety is complicated by the tendency of the monolithio *o*-carborane to disproportionate into *o*-carborane and its dianion [14]. Several strategies

have been followed to overcome this problem, for example, by using protecting/deprotecting methodologies, using dimethoxyethane as the solvent, or by doing the reaction at high dilution [15,16]. We recently revealed that mono and disubstitution of carboranes can be conveniently done in ethereal solvents at a very low temperature [17]. Such nucleophilic substitution methodology is perhaps the more general route for functionalizing carboranes as it can be applied to all carborane isomers.

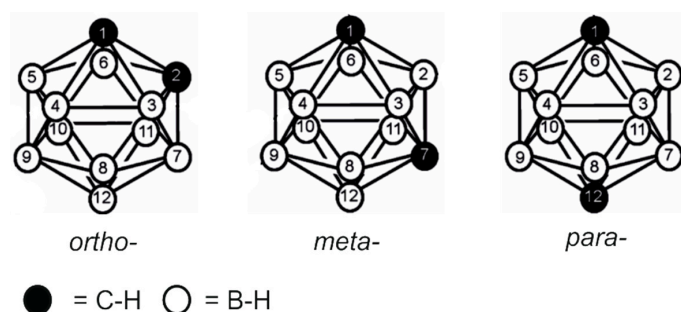


**Figure 1.** Graphical representation of the carborane isomers (*closo*-C<sub>2</sub>B<sub>10</sub>H<sub>12</sub>) with vertex numbering.

Over the years, our group and others have been interested in the synthesis of new carborane-based ligands containing a variety of donor centers (N, P, S, N/C, N/S, N/P, P/C, P/P, P/Si, P/S, S/C or S/S donors) and their metal complexes and applications [2,6,18–28]. Carborane ligands containing N,O donors are scarce in the literature. This is somewhat surprising when considering the importance of classical N,O-ligands in metal complexes and their properties [29–34]. One of the main objectives of our research in the last few years was to study the chemistry of carboranylmethylalcohols, particularly of those containing a heteroatom such as nitrogen, and exploring their properties. Our interest in N/O-functionalized carboranes primarily stems from our rationale that introducing a carborane moiety in the place of a conventional carbon-based moiety would strongly influence the coordination chemistry of such compounds, in addition to other relevant properties, such as higher stability, hydrophobicity, *etc.* Integration of carboranes in place of organic ring systems (typically benzene) is a very popular strategy to trigger desirable properties in (bio)medicine [7,8] but is much less exploited in chemistry or materials science [35].

In the present review, we summarize our results and the results of others on the synthesis, structure and reactivity of carboranyl ligands containing N,O-donor atoms and their metal complexes and properties. Metallacarborane complexes, incorporating one or more metal atoms within a polyhedral carborane cage structure, are excluded of the present review. For some recent reviews on metallacarboranes see references [36–41].

## 2. Carboranyl Compounds with N,O-Donor Functionalities and Properties

### 2.1. Closo-Carboranylmethylalcohols with Nitrogenated Aromatic Rings

Reported pyridine-type containing carboranyl-based N,O-donor compounds are summarized in Chart 1. Carboranyl methanols are easily available by the addition of lithiocarboranes to aldehydes or ketones. Using this methodology, a wide variety of mono substituted carboranyl methanol derivatives have been synthesized [42,43]. Following a similar procedure we [44–49] and others [50,51] have prepared an extensive series of new monosubstituted *o*-, *m*- and *p*-carboranylmethylalcohols bearing nitrogenated aromatic rings, by the addition of lithiocarboranes to the corresponding pyridylaldehydes (1–4, Chart 1 and Scheme 1). The addition of dilithiocarboranes to two equivalents of the corresponding aldehydes, under the same reaction conditions, provided a new series of disubstituted *o*- and *m*-carboranylmethylalcohols (5–6, Chart 1) [52,53]. This synthetic methodology allows the preparation of the compounds in good yields in gram quantities from one-pot reactions, starting from commercially available materials.

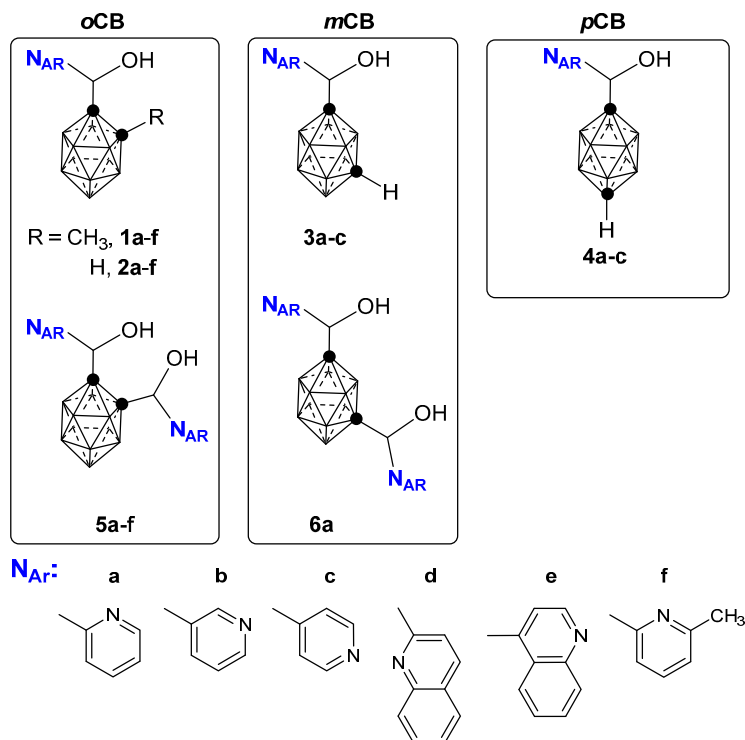
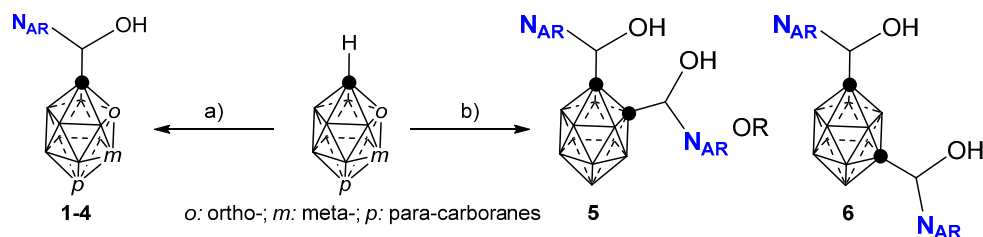
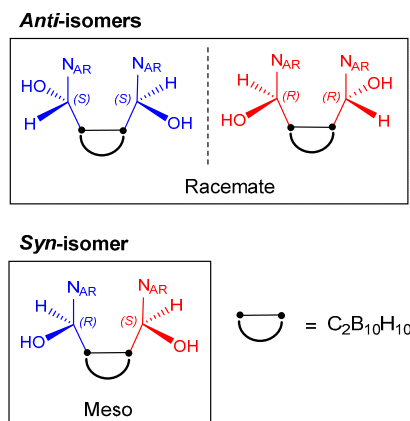


**Chart 1.** Synthesized carboranymethylalcohols with nitrogenated aromatic rings. *o*-, *m*- and *p*-CB refers to *ortho*-, *meta*- and *para*-carborane.



**Scheme 1.** General procedure for the syntheses of carboranymethylalcohols 1–6 (see Chart 1 for nomenclature). Conditions: (a) 1eq. *n*-BuLi, Ether/THF (0/−78 °C); 1eq. pyridine/quinolinecarboxaldehyde (−84/−63 °C); (b) 2eq. *n*-BuLi, Ether/THF (0 °C); 2eq. pyridinecarboxaldehyde (−94 °C for *o*CB or −63 °C for *m*CB).

This family of carboranymethylalcohols contains one (1–4; Chart 1) or two (5–6; Chart 1) chiral carbon centers. The monosubstituted compounds are therefore obtained as racemic mixtures, and they can be easily resolved into the *R* and *S* enantiomers by using HPLC over a chiral stationary phase [49,54], or by diastereomers formation with (1*S*)-(-)-camphanic acid chloride [50,51]. In the case of the disubstituted compounds (5–6), the situation is more complex (Scheme 2). These compounds contain two chiral centers that can adopt either *R* or *S* configuration and, therefore, lead to the formation of two diastereoisomers (Scheme 2), a *meso* compound (*RS*; OH groups in a *syn* orientation) and a racemic compound (mixture of *SS* and *RR*; OH groups in an *anti* orientation). The enantiopure compounds can be exploited in coordination chemistry, as will be described in the following sections. Separation of the *syn*- and *anti*-isomers in the disubstituted series of compounds has been carried out in the case of *o*-carborane derivatives 5a and 5b [53,55].



**Scheme 2.** Stereoisomers for chiral disubstituted carboranymethylalcohols.

Both mono and disubstituted carboranymethylalcohols mentioned above possess hydroxyl (OH) groups as hydrogen bond donors and nitrogen atoms that act as hydrogen bond acceptors. Indeed, the supramolecular chemistry of such compounds is dominated by moderate O–H...N hydrogen bonding. In the case of 2-pyridyl derivatives, **2a**, **3a** and **4b** (both in racemic and enantiopure forms), they all form homochiral helical networks and it has been shown that a correlation exists between the OCCN torsion angles of the molecules in the solid state and the handedness of the supramolecular helices [49]. Regarding the disubstituted derivatives, **5a–f**, it was observed that *syn* and *anti* stereoisomers crystallized separately from their mixtures and the detailed analysis of their supramolecular structures revealed that homochiral recognition seems to operate also in these molecular systems [53].

## 2.2. Other Closo-Carboranes Incorporating N and O Functionalities

Other reported non pyridine-type containing carboranyl-based N,O-donor compounds are summarized in Chart 2. A related family of compounds to that of **1–4** and **6** (Chart 1) is that of chiral carboranypyrroles **7–11** (Chart 2) [56]. In these molecules, the pyridyl moieties in the former ones are replaced by a pyrrol moiety. These carboranypyrroles were prepared by the reactions of mono or dialdehydes derivatives of *o*-, *m*- and *p*-carborane with pyrroles in the presence of acid catalysts (Scheme 3). Provided that the pyrrol moieties could be deprotonated, these compounds might provide rich coordination chemistry.

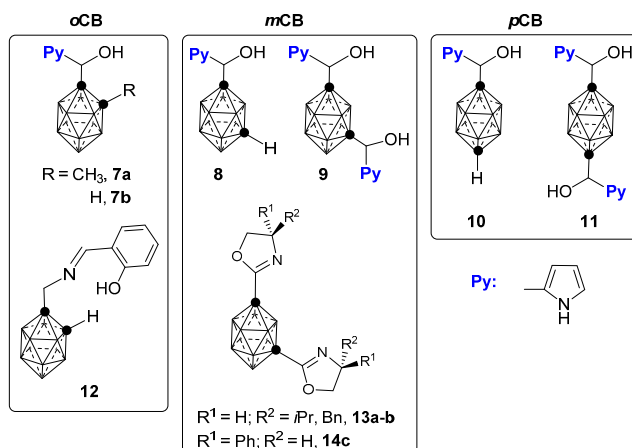
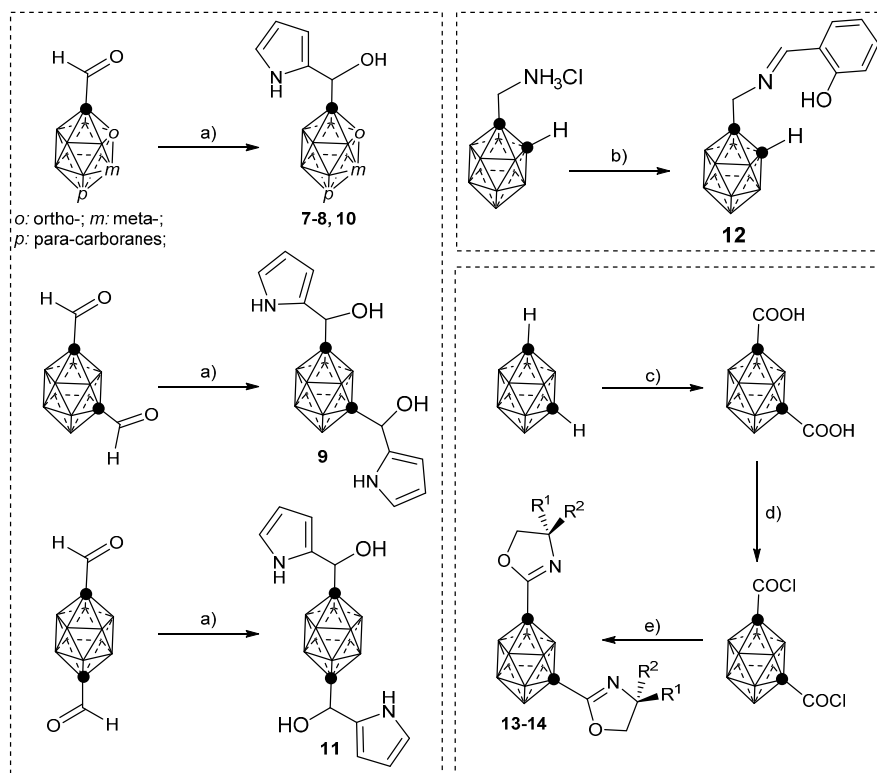


**Chart 2.** Other synthesized carboranes incorporating N and O functionalities. *o*-, *m*- and *p*-CB refers to *ortho*-, *meta*- and *para*-carborane.



**Scheme 3.** General procedure for the syntheses of carborane derivatives in Chart 2. Conditions: (a) pyrrole (excess), TFA or  $\text{InCl}_3$  ( $0\text{ }^\circ\text{C}$ ), 1 h; (b)  $\text{NaHCO}_3$ , 2-hydroxybenzaldehyde, toluene (reflux), two days; (c) *n*-BuLi, Ether,  $\text{CO}_2$ , HCl; (d)  $\text{SOCl}_2$  (reflux), 24 h; (e) 3 eq. DAST,  $\text{CH}_2\text{Cl}_2$  ( $-20\text{ }^\circ\text{C}$ ), 12 h.

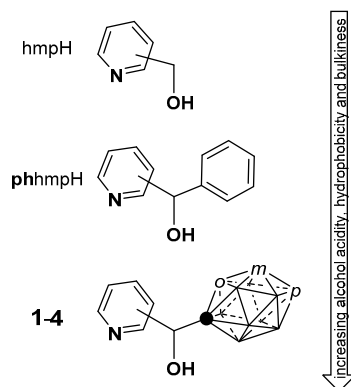
Reaction of *o*-carboranymethyl ammonium salt with commercially available phenyl aldehyde provided the phenyl(carboranymethyl)imine **12** (Chart 2 and Scheme 3) in good yield [57]. Another interesting series of compounds is that of chiral bis(oxazolidinyl)-*m*-carboranes **13–14** that were synthesized via a multistep synthesis [58]. Briefly, *m*-carborane dicarboxylic acid was transformed to the acyl chloride with  $\text{SOCl}_2$  and further condensed with two equivalents of the corresponding resolved amino alcohols to provide the uncyclized bis(hydroxyamide)-*m*-carborane intermediates. Double cyclization reaction by diethylaminosulfur trifluoride (DAST) afforded enantiopure compounds **13–14** in very high yields (Scheme 3).

### 3. Synthesis of Coordination Complexes and Properties

In the following, it will be shown the effect that the incorporation of carboranes has into the coordination chemistry of the otherwise carbon-based ligands (whenever possible) and the properties of such materials.

#### 3.1. Complexes of Monosubstituted **1–4** and **12**

Conventional N,O ligands such as (hydroxymethyl)pyridines (hmpH; Scheme 4) have proved to be successful building blocks for the self-assembly of metallocsupramolecular architectures with exciting physical properties [54] (and references therein). Carborane compounds **1–4** can be regarded as hmpH ligands where one of the H atoms at the  $-\text{CH}_2-$  position of the methylalcohol moiety has been replaced by a carboranyl fragment (Scheme 4). The introduction of carborane into the hmpH backbone provokes a bigger decrease of the alcohol *pK*<sub>a</sub> value, with respect to the related phenyl-hmpH (phhmpH) derivative (Scheme 4), in addition to an increase of the size and hydrophobicity of **1–4** with respect to phhmpH.

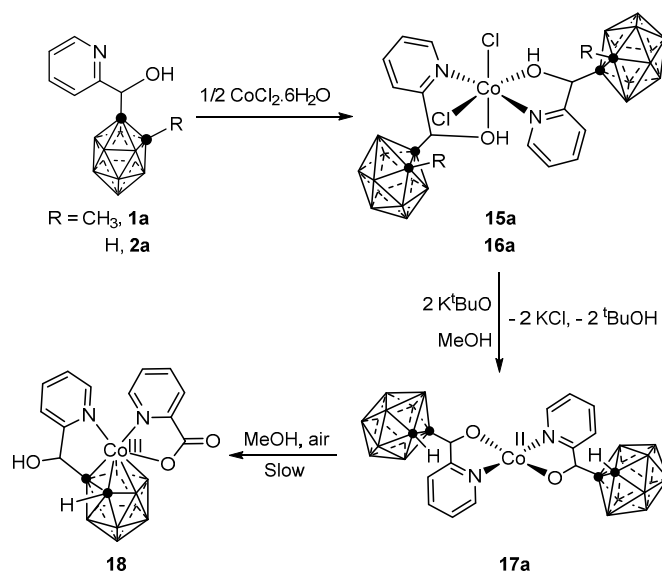


**Scheme 4.** Comparison of various pyridylmethanol derivatives.

Furthermore, the possibility for placement of the methylalcohol moiety at the 2-, 3- or 4-position with respect to the pyridine (or quinoline) nitrogen, which usually coordinates to the metal center, is a key feature that allows these ligands to support a whole family of supramolecules of a different nature. Heterobidentate ligands of this type offer several advantages over traditional symmetrical bidentate ligands by creating steric, electronic, asymmetry and chirality at the metal centers [59].

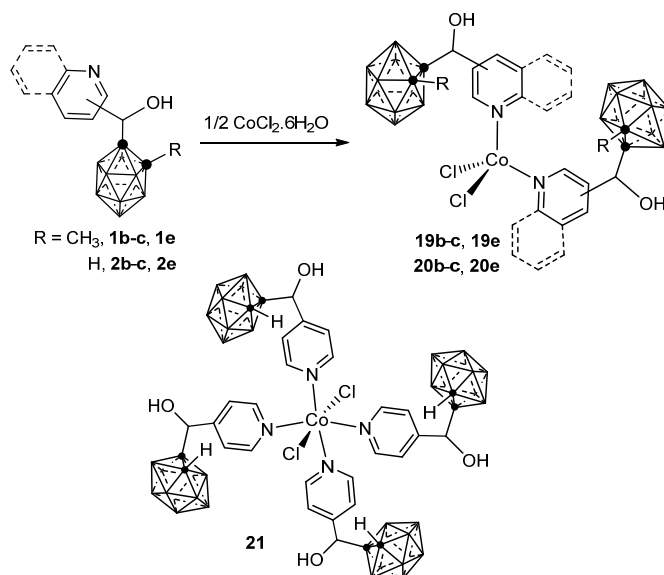
### 3.1.1. Cobalt

The 2-pyridyl derivatives **1a** and **2a** reacted with  $\text{CoCl}_2 \cdot 6\text{H}_2\text{O}$  in a 2:1 ratio under aerobic conditions to provide the corresponding  $\text{Co}^{\text{II}}$  complexes **15a** and **16a**, respectively (Scheme 5) [60]. X-ray diffraction studies confirmed that **2a** acts as a bidentate N,O-ligand, giving an octahedral-coordinated  $\text{Co}^{\text{II}}$  complex. We showed experimentally (both in solution and solid state) that the  $\text{Co-OH(R)}$  bonds in **16a** are labile and that the coordination strength of the alcohol function can be modulated by solvent-assisted intermolecular hydrogen bonding. We also showed that full deprotonation of both alcohol hydrogens in the octahedral cobalt complex **16a** afforded a rare square-planar  $\text{Co}^{\text{II}}$  complex **19a** that was characterized by single crystal X-ray diffraction (XRD). The square-planar geometry in this complex seemed to be induced by the steric hindrance generated by the carborane moiety on the ligand. Complex **17a** seems to enable  $\text{O}_2$  activation, followed by transformation of the ligands and metal oxidation states affording a  $\text{Co}^{\text{III}}$  carborane complex **18**.



**Scheme 5.** Syntheses of complexes 15–18.

The 3- and 4-pyridyl or quinolyl derivatives **1b–c**, **1e** and **2b–c**, **2e** also reacted with  $\text{CoCl}_2 \cdot 6\text{H}_2\text{O}$  under the same reaction conditions, providing, in this case, the corresponding tetrahedral  $\text{Co}^{\text{II}}$  complexes **15a** and **16a**, respectively (Scheme 6) [60]. Octahedral complex **21** was, however, formed in the presence of excess of **2c**. The structure for complexes **19c**, **19e**, **20b**, **20e** and **21** were confirmed by XRD.



Scheme 6. Syntheses of complexes 19–21.

It is interesting that even though the above  $\text{Co}^{\text{II}}$  complexes are paramagnetic, we were able to perform and characterize most of the complexes by NMR spectroscopy. The solid-state, variable-temperature (2–300 K) magnetic susceptibility data were collected on polycrystalline samples of **16a**, **20b** and **20c** (Figure 2) and the data agree well with their crystallographic data and stress the relevance of intermolecular interactions among neighboring molecules providing well-organized supramolecular 1 D systems (*vide infra*).

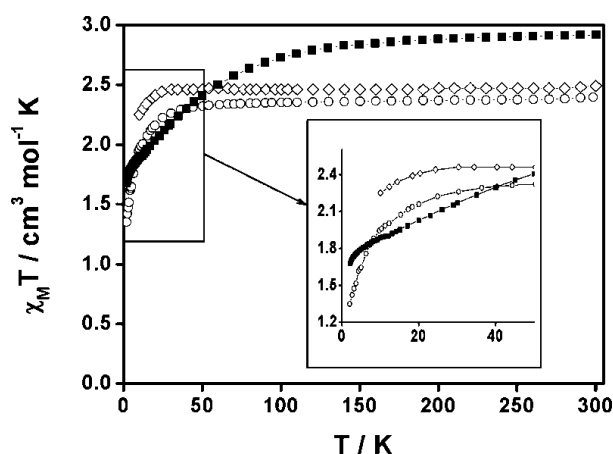
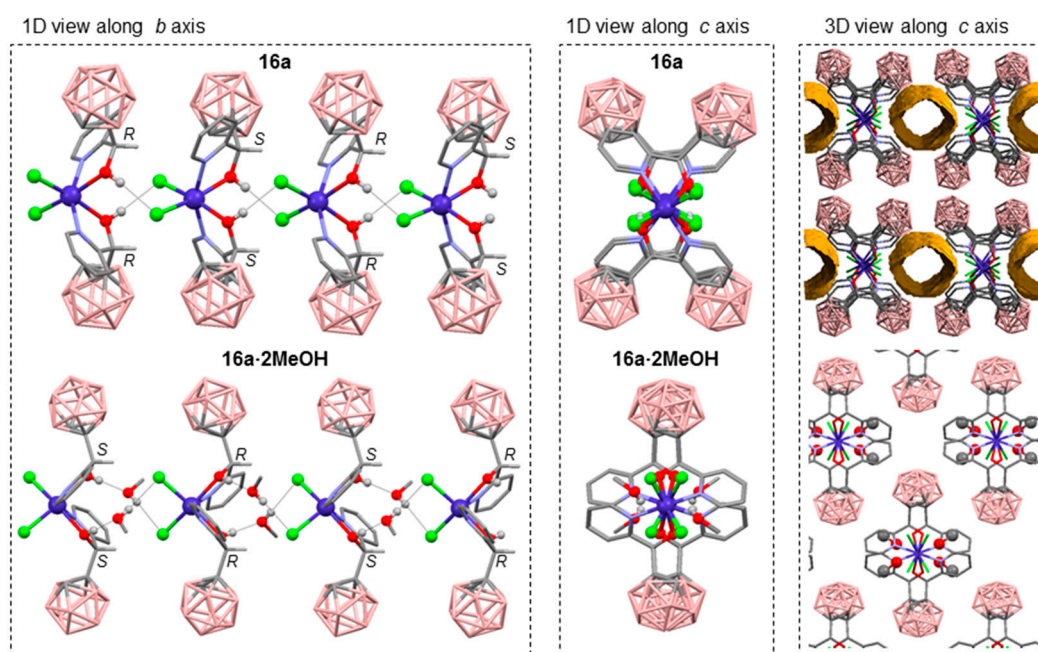


Figure 2.  $\chi_M T$  vs  $T$  plots for compound **16a** (black squares), **20b** (white circles) and **20c** (white rhombs) between 2.0 and 300.0 K. Inset: Increased section of the graph containing all three compounds from 2 to 50 K. Solid lines in  $\chi_M T$  vs.  $T$  plots are for eye guide.

In the solid state, all the above  $\text{Co}^{\text{II}}$  complexes show intermolecular  $\text{O-H}\cdots\text{Cl}/\text{O}$  hydrogen bonds. From those, unsolvated structures show exclusively  $\text{O-H}\cdots\text{Cl}$  hydrogen bonds giving supramolecular

chains. Those are, however, interrupted whenever an oxygen-containing solvent is included in the structures. In that case, O–H···O hydrogen bonds are also formed, interfering partially (**21**) or totally (**16a**) with the O–H···Cl hydrogen bonds. The supramolecular chemistry of **16a** serves as an example of this phenomena and of how the carborane moieties can have an influence on the solid structure and properties of the molecular complex. A comparison of the molecular and supramolecular structures of the octahedral complex **16a** with that of related (not containing carborane) cobalt complexes revealed that the chirality of **2a** in conjunction with the bulky carborane favors *RR/SS* alternation as a more economic packing arrangement. As shown at the top of Figure 3, the unsolvated form of **16a** gives chains, alternating *RR* and *SS* enantiomeric complexes, along the *c* axis via the O–H···Cl hydrogen bond interactions (Figure 3, top left). The proximity of the complexes (Co···Co: 5.722 Å) forces the carborane cages of consecutive molecules to be staggered (Figure 3, top middle). The solid structure significantly changed when **16a** was recrystallized from methanol. The methanol solvate of the latter, **16a**·2MeOH, also shows chains of alternating *RR* and *SS* enantiomeric complexes (Figure 3, bottom). However, two methanol molecules are inserted now in the hydrogen bonding network, resulting in a longer distance between consecutive Co centers (Co···Co: 7.281 Å) than in **16a**. As a consequence, the molecules in **16a**·2MeOH are not staggered but eclipsed (Figure 3, bottom). This has important consequences in the three-dimensional (3D) structures of these two complexes, as shown in Figure 3 (right column). The eclipsed chains in **16a**·2MeOH are more closely packed than the staggered chains in **16a** and as a consequence, the packing of stagger chains of **16a** creates defined channels running along the *c* axis parallel to hydrogen bonded chains (Figure 3, right). The solvation process from **16a** to **16a**·2MeOH has been demonstrated experimentally by exposing **16a** to liquid methanol, or even vapors.

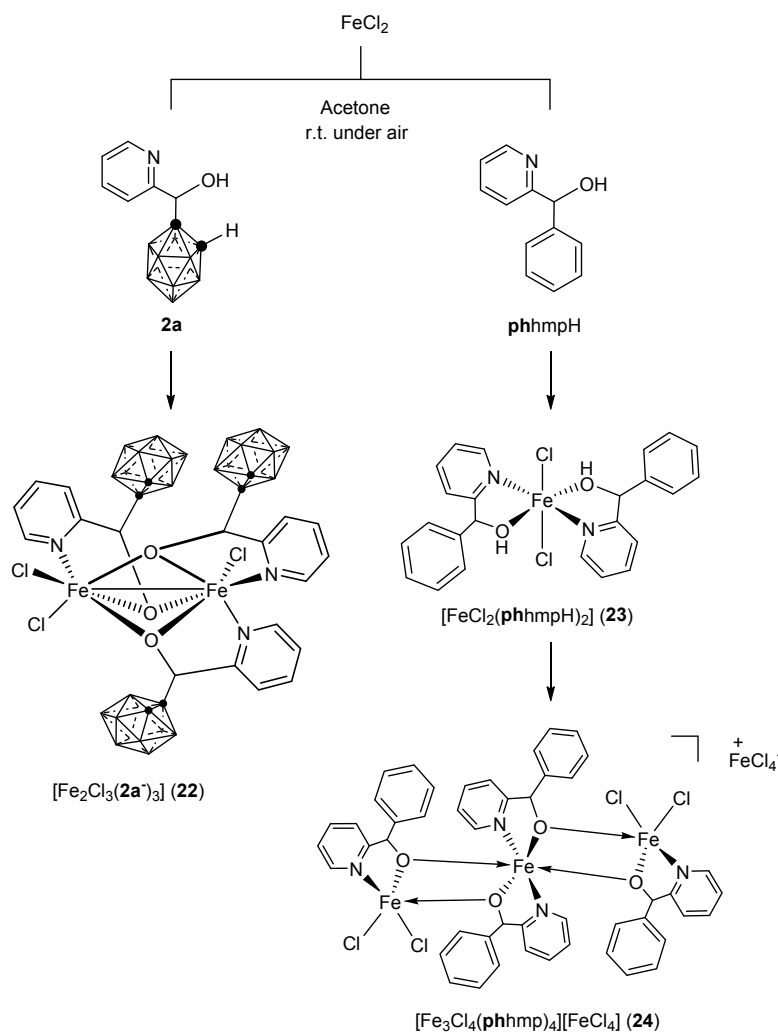


**Figure 3.** Supramolecular assemblies of **16a** and **16a**·2MeOH. Left column: Projections showing four molecules of each compound forming hydrogen-bonded chains. Middle column: Projections along the hydrogen-bonded chains showing a staggered arrangement of the carboranyl fragments in **16a** (top) versus an eclipsed arrangement in **16a**·2MeOH (bottom). Right column: A comparison of the 3D supramolecular assemblies of **16a** (left) and **16a**·2MeOH (right) showing the well-defined channels (yellow-orange) running along the *c* axis in the former and the absence of voids in the latter. All hydrogen atoms, except those for the CHOH group, are omitted for clarity. Color code: B pink; C grey; H white; O red; N light blue; Cl green; Co blue.



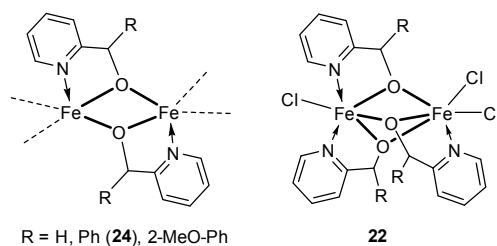
## 3.1.2. Iron

The reaction of **2a** with  $\text{FeCl}_2$  in a 1.5:1 ratio afforded the  $\text{Fe}^{\text{III}}$  complex  $\text{Fe}_2\text{Cl}_3(\mathbf{2a}^-)_3$  (**22**) in nearly quantitative yield (Scheme 7) [54]. When the same reaction was carried out with the phenyl-modified ligand **phhmpH**, initial formation of the mononuclear  $\text{Fe}^{\text{II}}$  complex  $\text{FeCl}_2(\text{phhmpH})_2$  (**23**) was observed, followed by its conversion to the trinuclear  $\text{Fe}^{\text{III}}$  complex  $[\text{Fe}_3\text{Cl}_4(\text{phhmp})_4][\text{FeCl}_4]$  (**24**). Structures for complexes **22**–**24** have been solved by XRD. It was observed that deprotonation occurred spontaneously in the reactions of **2a** with iron, but this was faster in the case of the carborane-based ligand **2a** than with the phenyl-based one **phhmpH**, in agreement with a higher acidity for **2a**.



Scheme 7. Syntheses of complexes **22**–**24**.

These results clearly showed how the introduction of the bulky *o*-carborane into the 2-(hydroxymethyl)pyridine (hmpH) architecture significantly alters the coordination of the simple or arylsubstituted 2-hmpH. The comparison of **22** with all other  $\text{Fe}^{\text{III}}$  complexes in the literature having arylsubstituted 2-hmpH ligands revealed that the latter always show two alkoxide pyridylalcohol ligands bridging two close  $\text{Fe}^{\text{III}}$  ions (Scheme 8), whereas the dinuclear complex **22** contains three alkoxide bridges. This unusual architecture seems to be triggered by the poor nucleophilicity of the alkoxide ligand ( $\mathbf{2a}^-$ ).



**Scheme 8.**  $\mu_2$ -O versus  $\mu_3$ -O bridging of hmpH in Fe complexes.

The presence of three alkoxide bridges in **22** is rather surprising, owing to the size of the carborane cages, and it has important structural consequences. Each of the pyridylalcohol ligands can adopt an *R* or *S* configuration, so that *RRR*, *SSS*, *RRS* and *SSR* could all be expected in complex **22**. However only *RRS* and/or *SSR* combinations are possible due to the steric hindrance imposed by the same hardness of the ligands (**22**·acetone, Figure 4). This was confirmed by synthesizing the enantiopure complexes of **22** from pure *R* and *S* enantiomers of **2a**. The chirality of the enantiopure ligands ((*R*)-(+)-**2a**/((*S*)-(–)-**2a**) and corresponding complexes (*S,S*) $A^{Fe}(R)A^{Fe-}(+)$ -**22** and (*R,R*) $C^{Fe}(S)C^{Fe-}(-)$ -**22** was confirmed by circular dichroism (CD) measurements in solution and by second-harmonic generation (SHG) measurements in the solid state (Figure 5).

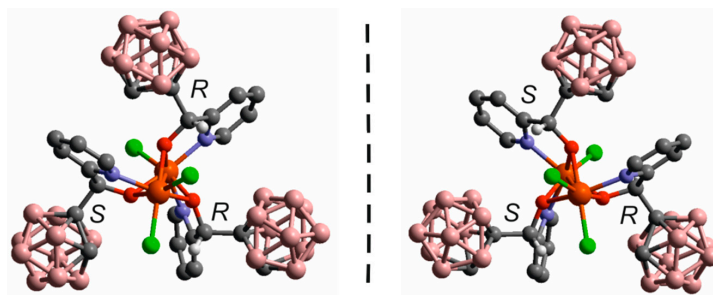


**Figure 4.** Ball and stick representation of the molecular structure of **22**·acetone showing both enantiomers in the racemate; All hydrogen atoms, except those for the CHOH group, are omitted for clarity. Blue = N, pink = B, dark Grey = C, Orange = Fe.

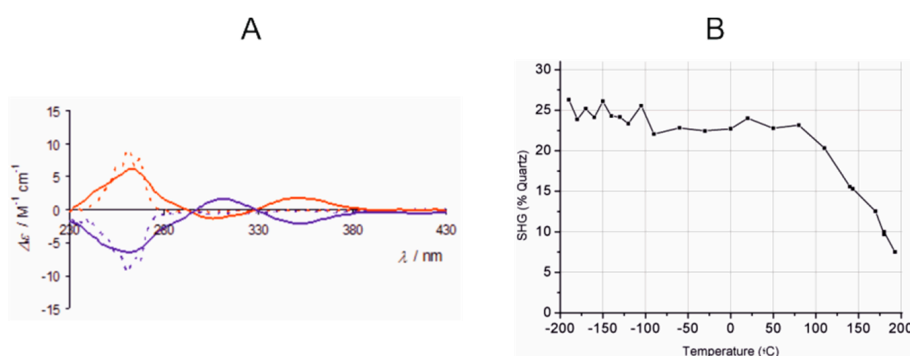


**Figure 5.** (A) CD spectra of *R*(+)-**2a** (blue dotted lines), *S*(–)-**2b** (red dotted lines), (*R,R*) $C^{Fe}(S)C^{Fe-}(-)$ -**22** (blue plain lines) and (*S,S*) $A^{Fe}(R)A^{Fe-}(+)$ -**22** (red plain lines); (B) SHG Intensity of a mixture of (*R,R*) $C^{Fe}(S)C^{Fe-}(-)$ -**22** and (*S,S*) $A^{Fe}(R)A^{Fe-}(+)$ -**22** versus temperature between –200 °C and 200 °C.

The crystalline powder obtained during the synthesis of **22** was identified as a racemic mixture of (*S,S*) $A^{Fe}(R)A^{Fe-}(+)$ -**22** and (*R,R*) $C^{Fe}(S)C^{Fe-}(-)$ -**22** by Powder X-ray Diffraction (PXRD). This racemic mixture (*rac*-**22**) showed a very rare case of spontaneous resolution that takes place on precipitation or exposition to vapors giving a conglomerate compound (*co*-**22**), as shown in Figure 6.

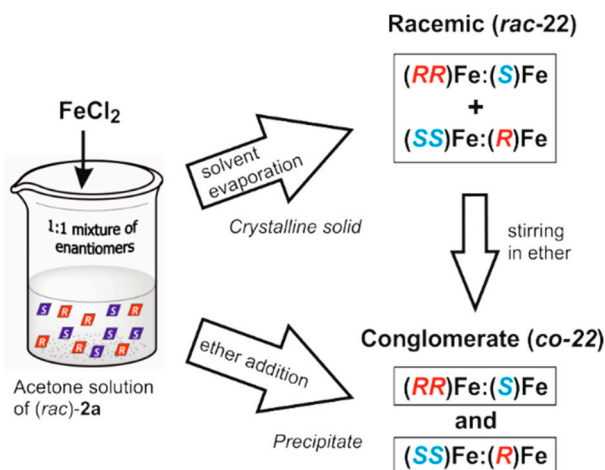


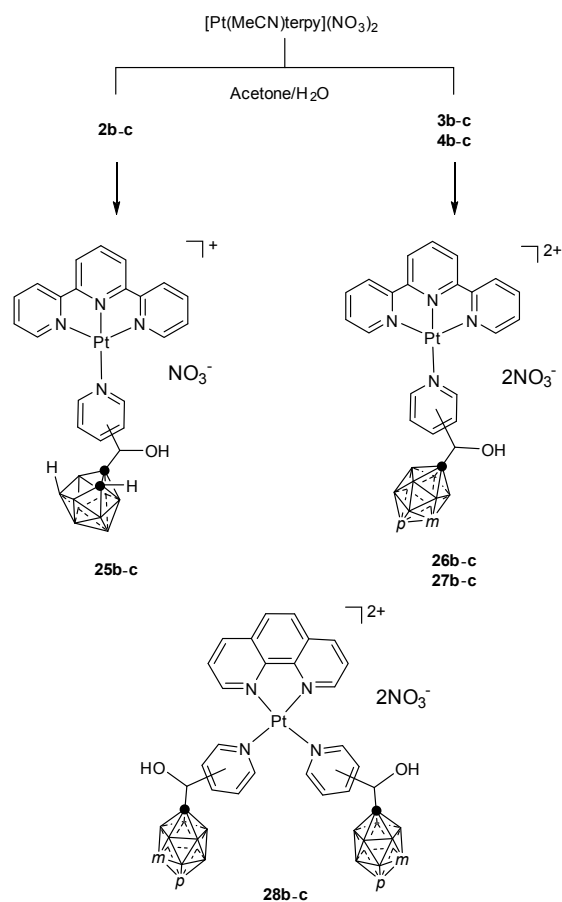
**Figure 6.** Schematic representation of racemic (*rac*-22) and conglomerate (*co*-22) formation for bulk samples of 22.

Complex 22 constitutes the first dinuclear Fe<sup>III</sup> system containing three alkoxide bridges that displays an antiferromagnetic behavior. DFT calculations have corroborated the latter and show that the Fe–O distance is the main parameter that controls the magnetic behavior. Overall, complex 22 represents an interesting class of multifunctional molecular materials that combine magnetic, chiroptical and second-order optical properties.

### 3.1.3. Platinum

Contrary to the above metals, when a Group 10 metal such as Platinum was employed, only N-coordination was observed. Reactions of racemic 2c and/or enantiopure 3b–c/4b–c with [Pt(MeCN)terpy](NO<sub>3</sub>)<sub>2</sub> or [PtI<sub>2</sub>(phen)] provided the platinum complexes 25b–c, 26b–c, 27b–c or 28b–c (Scheme 9) [51,61]. Recrystallization of the complexes 25b–c, 26b–c and 27b–c from hot water was necessary in order to remove the byproduct [Pt(OH)terpy]NO<sub>3</sub>. Under such conditions, the *o*-carborane ligands 2b–c were deboronated to the corresponding 7,8-*nido*-carboran-7-yl)pyridylmethanol complexes 25b–c. Deboronation was not observed in any of the *m*- or *p*-carborane derivatives, consistent with their higher stability. The deboronation of *o*-carborane-containing ligands is known to be enhanced when coordinated to metal centers [62–66]. The phenomenon is attributed to the electron density being withdrawn from the boron cluster upon metal complexation. There are, however, some reports, mainly dealing with Pt<sup>II</sup> complexes where deboronation seems to occur prior to metal complexation and most probably due to the nucleophilicity of the ligand itself [67,68].

The use of β-cyclodextrin (CD) as biodelivery agents for carborane clusters is of particular relevance to their exploitation as unique hydrophobic pharmacophores in medicinal chemistry [7,8]. Chiral complexes 26b–c and 27–c form water-soluble supramolecular 1:1 host-guest β-CD adducts [51]. The nature of the carborane cage itself (*i.e.*, the positional isomer and the overall charge) and the chirality and nature of the substituent on the cage each contribute to its molecular recognition by β-CD. S–27c forms a remarkably stable ternary system, involving, simultaneously, DNA metallointercalation and β-CD encapsulation (Figure 7). Complexes 28b–c, containing two *closo*-carborane clusters, were also treated with β-CD to provide the corresponding series of water-soluble 2:1 host-guest adducts [61]. DNA-binding studies demonstrated the avid binding affinity of these complexes for calf thymus DNA.



Scheme 9. Syntheses of complexes 25–28.

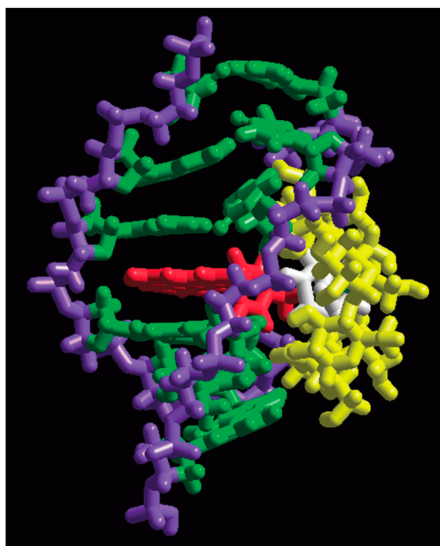
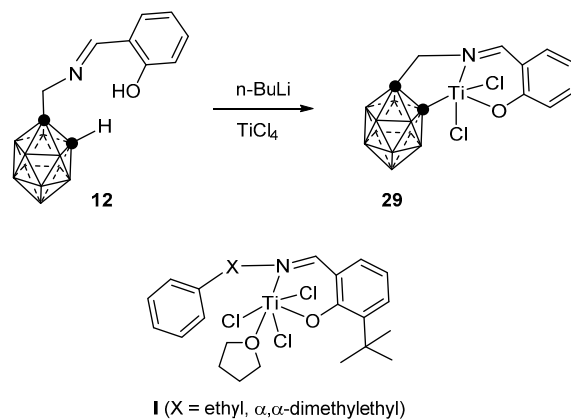


**Figure 7.** Model showing the ternary structure with intercalation of *S*-27c- $\beta$ -CD from the major groove of the hexanucleotide. The d(GTCGAC)<sub>2</sub> residues are depicted in green and the phosphodiester/ribose backbones in purple. The platinum(II)-terpy complex is depicted in red, the carborane cage is white, and the  $\beta$ -CD is yellow. Reproduced from Reference [50] with permission of The Royal Society of Chemistry.

### 3.1.4. Titanium

*In situ* deprotonation of **12** followed by reaction with  $\text{TiCl}_4$  afforded complex **29** (Scheme 10) [57]. This complex is an efficient catalyst for  $\alpha$ -olefin polymerization to produce high molecular weight polyethylene and poly(ethylene/methyl-10-undecanoate). Catalytic activity of complex **29** is clearly superior to that of **I** (bottom Scheme 10) [69] and comparable to one of the most potent phenoxy–imine Ti complexes (Ti-FI catalysts) [70].



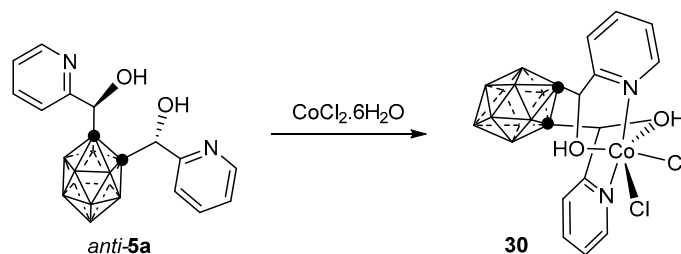
Scheme 10. Synthesis of complex **29**.

### 3.2. Complexes of Disubstituted **5–6** and **13–14**

The 2-pyridyl disubstituted *closo*-carboranymethyl alcohols **5–6** (Chart 1) or **13–14** (Chart 2), constitute a second generation of ligands, where two pyridyl/quinolylmethylalcohol or oxazolinyll chiral moieties radiate out of the cluster carbon atoms. The presence of two chiral carbons and the different positional isomers offer enough molecular diversity to explore the coordination chemistry of such ligands.

#### 3.2.1. Cobalt

Racemic *anti*-**5a** (see Scheme 2 for nomenclature) formed the octahedral cobalt<sup>II</sup> complex **30** upon reaction with  $\text{CoCl}_2$  (Scheme 11) [71]. The X-ray structure of **30** revealed a distorted geometry where each cobalt<sup>II</sup> center is coordinated by all nitrogen and oxygen atoms of an *anti*-diastereomer of **5a** that is acting as a tetradentate  $\text{N}_2\text{O}_2$ -ligand. Crystals for the  $\text{Co}^{\text{II}}$  complex are formed by a racemic mixture of  $\Delta$ -**30** and  $\Lambda$ -**30** units.



Scheme 11. Synthesis of complex **30**.

The OH groups from *anti*-**5a** remained intact in complex **30** and therefore they can act as proton donors for hydrogen bonding and were also observed in complex **16a** (Scheme 3 and Figure 3). Complex **30** forms homochiral ribbons ( $\Delta$ - or  $\Lambda$ -enantiomeric complexes), along the *b* axis via O–H...Cl hydrogen bond interactions (Figure 8). Thus, homochiral recognition seems to be happening in the  $\text{Co}^{\text{II}}$  complexes of *anti*-**5a**.

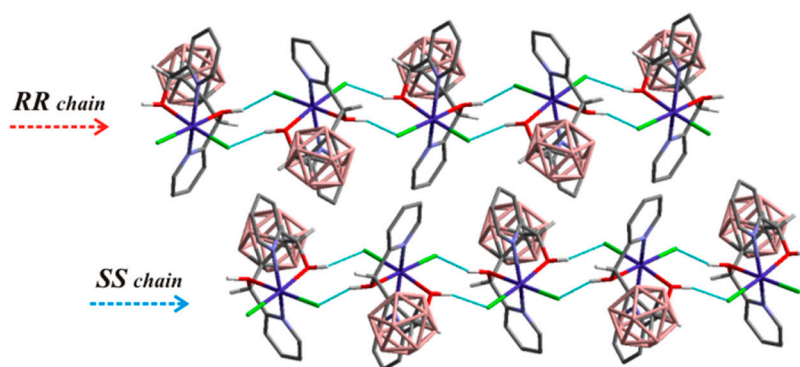


**Figure 8.** Supramolecular assembly of **30** showing two hydrogen-bonded homochiral ribbons (enantiomers indicated with arrows). All hydrogen atoms, except those for the CHOH group, are omitted for clarity. Blue = N, red = O, pink = B, dark grey = C, violet = Co, green = Cl.

We showed that *anti-5a* is an unprecedented and distinct tetradentate  $N_2O_2$ -type ligand and represents a new type of  $C_2$ -symmetric chiral building block. Reported tetradentate  $N_2O_2$  ligands are mainly reduced to Schiff-base backbone ligands [72–74]. These ligands and their derivatives coordinate predominantly in a planar arrangement to various metal ions giving *trans* geometries in octahedral complexes (Figure 9). An increased propensity to form *cis* structures has been achieved in some cases by increasing the backbone chain length. Carborane-based *anti-5a* ligand adopts preferentially a *cis- $\alpha$*  configuration around the  $Co^{II}$  center (Figure 9) and it is, therefore, able to produce chiral-at-metal complexes.

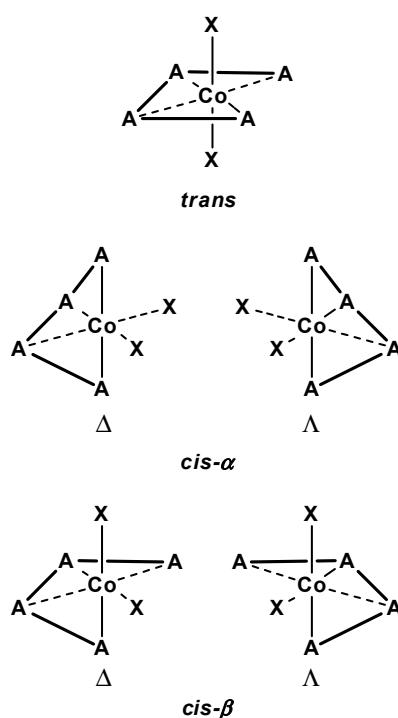
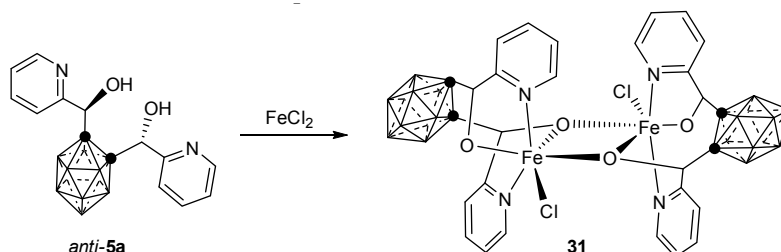


**Figure 9.** Octahedral-based geometric isomers for not branched tetradentate ligand.

### 3.2.2. Iron

The reaction of *anti-5a* with  $FeCl_2$  provided the dinuclear iron<sup>III</sup> complex **31** (Scheme 12) [55]. *Anti-5a* behaves also as a distinct tetradentate  $N_2O_2$  ligand, as already observed in the previous Co complex **30** and confirms this ligand as a new type of  $C_2$ -symmetric chiral building block.

X-ray structural analysis reveals that the alcohol groups are deprotonated, as already observed also in the iron<sup>III</sup> complex **22** (Scheme 5, Figure 4). As in the case of complex **30**, the crystallization of homochiral dimers in **31** suggests that enantiomeric forms of racemic *anti*-**5a** self-recognize to form exclusively stereospecific, homochiral dinuclear complexes.



Scheme 12. Synthesis of complex **31**.

The coordination chemistry of the *meso* form of **5a** (*syn*-**5a**; see Scheme 2 for nomenclature) resulted in being more complicated than that of the chiral *anti*-form, probably as a result of the *syn*-arrangement of the OH groups. After several attempts, the dinuclear iron<sup>III</sup> complex **33** crystallized and showed an unusual dinuclear iron<sup>III</sup> complex with a mixed octahedral and square pyramidal geometry (Figure 10).

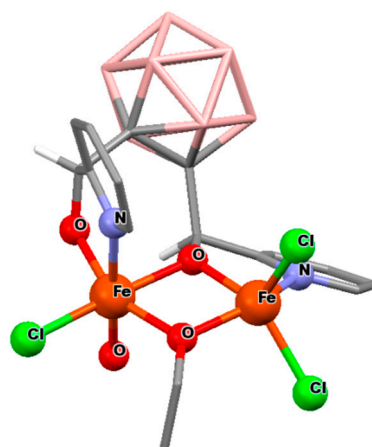


Figure 10. Molecular structure of  $\text{Fe}_2\text{Cl}_3(\text{syn-5a}^{2-})(\text{EtO})(\text{H}_2\text{O})$  (**31**). All hydrogen atoms, except those for the CHOH group, are omitted for clarity. Pink = B, dark Grey = C.

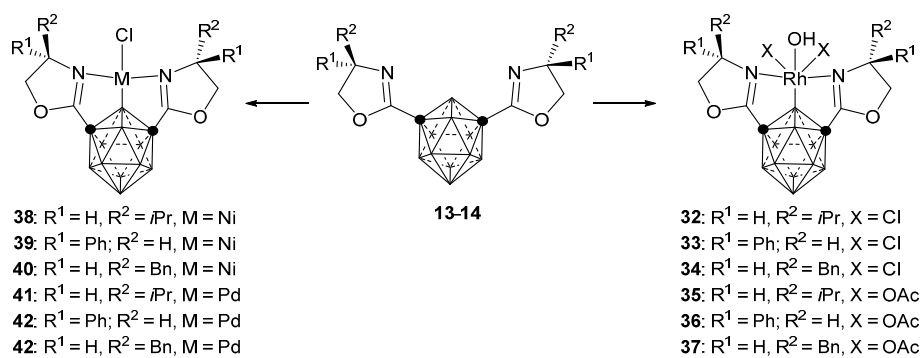
Complex **31** could be obtained in the solid state as a single phase, and the solid-state, variable-temperature (2–300 K) magnetic susceptibility data using 0.03 and 0.5 T fields were measured. It was found that an exchange coupling for both Fe<sup>III</sup> atoms in **31** was strongly antiferromagnetic.

### 3.2.3. Nickel, Palladium and Rhodium Complexes

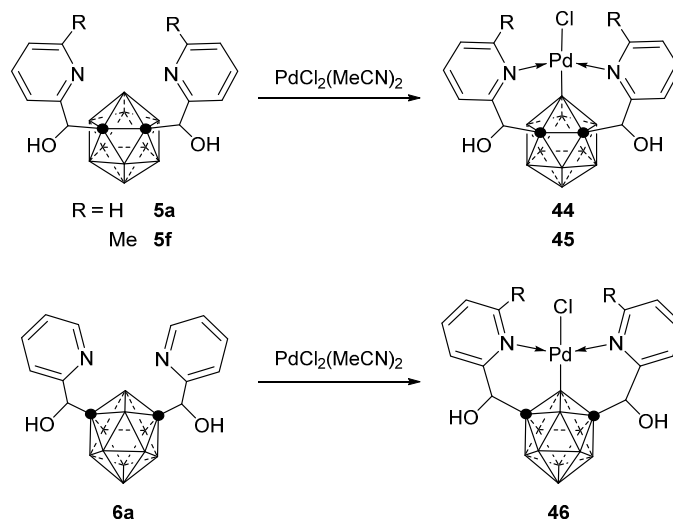
Chiral NBN pincer complexes of disubstituted enantiopure oxazolynyl *m*-carboranes **13–14** (Chart 2), were prepared by their reaction with  $\text{RhCl}_3 \cdot 3\text{H}_2\text{O}$ ,  $[\text{Ni}(\text{COD})_2]$  or  $[\text{Pd}(\text{MeCN})_4](\text{BF}_4)_2$  under heating conditions (Scheme 13) [58]. Chiral rhodium complexes **32** (chloride form) and **35** (acetate form) were found to be an effective catalyst (1 mol%) for asymmetric conjugate reaction of  $\alpha,\beta$ -unsaturated esters, giving both a high enantiomeric excess (93%–94% ee). Lower ee were obtained with complexes **36** and **37**. The enantioselectivities were similar to those obtained with the Phebox pincer complex, having a phenyl ring in place of the *m*-carborane (Scheme 13) [75]. Complexes **35–37** were also found to be active catalysts for the asymmetric reductive aldol reaction of

benzaldehyde, *tert*-butyl acrylate and  $(\text{EtO})_2\text{MeSiH}$ . In this case, the ee was sensibly higher (91% ee) than the corresponding Phebox pincer complexes (77%–87% ee) [76].

Reaction of the disubstituted 2-pyridyl *closo*-carboranymethyl alcohols **5a**, **5f** and **6a** (Chart 1) with  $[\text{PdCl}_2(\text{MeCN})_2]$  provided the pincer palladium complexes **44**–**46**, respectively, under mild conditions (Scheme 14) [52]. XRD of these complexes show unambiguously B–H activation of the carborane cages at B(3/6)H in *o*-carborane or B(2/3)H in the *m*-carborane-based ligands. The structures of the three complexes displayed exceptionally long Pd–Cl distances in the solid state (2.49–2.51 Å), suggesting a strong *trans* influence of the carborane moieties and comparable with that for alkyl-based pincer Pd complexes (2.49–2.52 Å). However, a combined study of experimental and calculated bond distances reveals that two effects are operative in modulating the Pd–Cl distance in the crystal structures. One is the *trans* influence of the carborane moieties, the other being the intermolecular moderate H-bonding interactions among neighboring complexes in the solid state. Thus, it can be inferred that there is a stronger *trans* influence of the *meta*-carborane than the *ortho*-carborane moieties in the pincer complexes, as expected.



Scheme 13. Syntheses of complexes 32–42.



Scheme 14. Syntheses of complexes 44–46.

Catalytic applications of **44** and **46** have shown the complexes are good catalyst precursors in Suzuki coupling reactions in water, and with remarkably low amounts of catalyst loadings (0.0001 mol %) and good functional group tolerance for the substrates. Complex **44** shows a better catalytic profile than **46** and with excellent conversions and TON values ranging from 770,000 to 990,000, thus showing a very high catalytic activity which rivals previous reports on Suzuki coupling performed by very low amounts of palladium catalysts, even with other pincer complexes [52].



#### 4. Conclusions and Perspectives

The coordination chemistry of N,O-type carborane-based ligands with  $\text{Ti}^{\text{IV}}$ ,  $\text{Fe}^{\text{III}}$ ,  $\text{Co}^{\text{II}}$ ,  $\text{Rh}^{\text{III}}$ ,  $\text{Ni}^{\text{II}}$ ,  $\text{Pd}^{\text{II}}$ ,  $\text{Pt}^{\text{II}}$  and  $\text{Zn}^{\text{II}}$  has been summarized, along with the properties and applications of these metal complexes. The above results nicely expand the already rich carborane chemistry and show how introduction of the carborane framework into the otherwise conventional carbon-based ligands, opens up new avenues in coordination chemistry with exciting metal-mediated reactivity and properties. The convenient preparation of N,O-type carborane-based compounds, many of them in one-pot reaction and from commercially available starting materials, make of these carborane derivatives valuable ligands for coordination chemistry. The diverse coordination modes of such ligands towards a variety of metals and their properties are all advantageous. The pyridine-containing *o*-carboranylmethyl alcohol ligands **1–4** (Chart 1) are analogous to the (hydroxymethyl)pyridines (hmpH; Scheme 2), or other derivatives of the latter. It has been, however, demonstrated that the replacement of an H atom or a phenyl ring by a carboranyl moiety in these systems has an enormous influence on the final metal complexes and properties. This led to the formation of a dinuclear chiral iron complex combining magnetic, chiroptical and second-order optical nonlinear properties. The same complex showed a fascinating case of spontaneous resolution on precipitation or exposition to vapors. It has been described how the carborane moieties triggered the porosity of an antiferromagnetic  $\text{Co}^{\text{II}}$  complex. Platinum complexes incorporating *o*-carboranylmethyl alcohol ligands formed supramolecular host-guest  $\beta$ -CD and/or DNA adducts. Titanium, nickel, palladium and rhodium complexes provided active catalysts for a variety of chemical transformations such as polymerization, enantioselective asymmetric conjugate reaction of  $\alpha,\beta$ -unsaturated esters or aldol reactions, and Suzuki coupling reactions in water and with very low catalytic loadings.

Another area of interest is that of chirality, as some of the present N,O-ligands are chiral and can be easily obtained in enantiopure forms. This will certainly facilitate the use of such chiral ligands and their corresponding complexes in NLO, ferroelectric or multifunctional materials. This review highlights the versatility of carboranes as alternatives to carbon-based ligands in metal complexes for solving problems that might spoil their applicability, such as, e.g., thermal or water stability, or just by improving the activity or selectivity of catalysts. Boron chemistry in general, and carborane chemistry in particular, is nowadays a very mature and established area of research. New developments are appearing constantly and are limited only by our imagination.

**Acknowledgments:** We thank MEC grants CTQ2013-44670-R, MAT2013-47869-C4-2-P and Generalitat de Catalunya 2014/SGR/00149 for financial support. We would like to thank and dedicate this review to the people and key players in the papers of our group; their work has wonderfully influenced our research in the past few years.

**Author Contributions:** Francesc Teixidor and Clara Viñas contributed to the critical reading and discussion of the review contents; José Giner Planas wrote the paper.

**Conflicts of Interest:** The authors declare no conflict of interest.

#### References

1. Grimes, R.N. *Carboranes*, 2nd ed.; Academic Press: Oxford, UK, 2011.
2. Teixidor, F.; Viñas, C. *Science of Synthesis*; Thieme: Stuttgart, Germany, 2005; Volume 6, p. 1325.
3. Hermansson, K.; Wójcik, M.; Sjöberg, S. *o*-, *m*-, and *p*-Carboranes and Their Anions: Ab Initio Calculations of Structures, Electron Affinities, and Acidities. *Inorg. Chem.* **1999**, *38*, 6039–6048. [[CrossRef](#)] [[PubMed](#)]
4. Grimes, R.N. Carboranes in the chemist's toolbox. *Dalton Trans.* **2015**, *44*, 5939–5956. [[CrossRef](#)] [[PubMed](#)]
5. Olid, D.; Núñez, R.; Viñas, C.; Teixidor, F. Methods to produce B–C, B–P, B–N and B–S bonds in boron clusters. *Chem. Soc. Rev.* **2013**, *42*, 3318–3336. [[CrossRef](#)] [[PubMed](#)]
6. Zhu, Y.H.; Hosmane, N.S. Carborane-based transition metal complexes and their catalytic applications for olefin polymerization: Current and future perspectives. *J. Organomet. Chem.* **2013**, *747*, 25–29.
7. Issa, F.; Kassiou, M.; Rendina, L.M. Boron in Drug Discovery: Carboranes as Unique Pharmacophores in Biologically Active Compounds. *Chem. Rev.* **2011**, *111*, 5701–5722. [[CrossRef](#)] [[PubMed](#)]

8. Scholz, M.; Hey-Hawkins, E. Carboranes as Pharmacophores: Properties, Synthesis, and Application Strategies. *Chem. Rev.* **2011**, *111*, 7035–7062. [[CrossRef](#)] [[PubMed](#)]
9. Dash, B.P.; Satapathy, R.; Maguire, J.A.; Hosmane, N.S. Polyhedral boron clusters in materials science. *New J. Chem.* **2011**, *35*, 1955–1972. [[CrossRef](#)]
10. Hardie, M.J. The use of carborane anions in coordination polymers and extended solids. *J. Chem. Crystallogr.* **2007**, *37*, 69–80. [[CrossRef](#)]
11. Grimes, R.N. Metallacarboranes in the new millennium. *Coord. Chem. Rev.* **2000**, *200–202*, 773–811. [[CrossRef](#)]
12. Adams, G.B.; O’Keeffe, M.; Ruoff, R.S. Van der Waals surface areas and volumes of fullerenes. *J. Phys. Chem.* **1994**, *98*, 9465–9469. [[CrossRef](#)]
13. Fauchère, J.L.; Do, K.Q.; Jow, P.Y.C.; Hansch, C. Unusually strong lipophilicity of “fat” or “super” amino-acids, including a new reference value for glycine. *Experientia* **1980**, *36*, 1203–1204. [[CrossRef](#)] [[PubMed](#)]
14. Zakharkin, L.I.; Grebennikov, A.V.; Kazantsev, A.V. Alkylation of carborane grignard reagents. *Bull. Acad. Sci. USSR Div. Chem. Sci.* **1968**, *16*, 1991–1993. [[CrossRef](#)]
15. Viñas, C.; Benakki, R.; Teixidor, F.; Casabo, J. Dimethoxyethane as a Solvent for the Synthesis of C-Monosubstituted *o*-Carborane Derivatives. *Inorg. Chem.* **1995**, *34*, 3844–3845. [[CrossRef](#)]
16. Gomez, F.A.; Hawthorne, M.F. A simple route to C-monosubstituted carborane derivatives. *J. Org. Chem.* **1992**, *57*, 1384–1390. [[CrossRef](#)]
17. Popescu, A.R.; Musteti, A.D.; Ferrer-Ugalde, A.; Viñas, C.; Núñez, R.; Teixidor, F. Influential role of ethereal solvent on organolithium compounds: The case of carboranyl lithium. *Chem. Eur. J.* **2012**, *18*, 3174–3184. [[CrossRef](#)] [[PubMed](#)]
18. Yao, Z.-J.; Deng, W. Half-sandwich late transition metal complexes based on functionalized carborane ligands. *Coord. Chem. Rev.* **2016**, *309*, 21–35. [[CrossRef](#)]
19. Popescu, A.R.; Teixidor, F.; Viñas, C. Metal promoted charge and hapticities of phosphines: The uniqueness of carboranyl phosphines. *Coord. Chem. Rev.* **2014**, *269*, 54–84. [[CrossRef](#)]
20. Yao, Z.J.; Jin, G.X. Transition metal complexes based on carboranyl ligands containing N, P, and S donors: Synthesis, reactivity and applications. *Coord. Chem. Rev.* **2013**, *257*, 2522–2535. [[CrossRef](#)]
21. Spokoyny, A.M.; Machan, C.W.; Clingerman, D.J.; Rosen, M.S.; Wiester, M.J.; Kennedy, R.D.; Stern, C.L.; Sarjeant, A.A.; Mirkin, C.A. A coordination chemistry dichotomy for icosahedral carborane-based ligands. *Nat. Chem.* **2011**, *3*, 590–596. [[CrossRef](#)] [[PubMed](#)]
22. Crespo, O.; Gimeno, M.C.; Laguna, A. Carboranyl C- $\sigma$ -bonded and C-functionalized carboranes as ligands in gold and silver chemistry. *J. Organomet. Chem.* **2009**, *694*, 1588–1598. [[CrossRef](#)]
23. Kang, S.O.; Ko, J. Chemistry of *o*-carboranyl derivatives. In *Advances in Organometallic Chemistry*; Academic Press: Cambridge, MA, USA, 2001; Volume 47, pp. 61–99.
24. Crespo, O.; Gimeno, M.C.; Laguna, A. Bis(diphenylphosphino)-ferrocene or -dicarba-closo-dodecaborane as ligands in gold and silver chemistry. *Appl. Organomet. Chem.* **2000**, *14*, 644–652. [[CrossRef](#)]
25. Teixidor, F.; Viñas, C.; Demonceau, A.; Núñez, R. Boron clusters: Do they receive the deserved interest? *Pure Appl. Chem.* **2003**, *75*, 1305–1313. [[CrossRef](#)]
26. Teixidor, F.; Núñez, R.; Flores, M.A.; Demonceau, A.; Viñas, C. Forced exo-nido rhoda and ruthenacarboranes as catalyst precursors: A review. *J. Organomet. Chem.* **2000**, *614–615*, 48–56. [[CrossRef](#)]
27. Teixidor, F.; Flores, M.A.; Viñas, C.; Sillanpää, R.; Kivekäs, R. Exo-nido-Cyclooctadienerrhodacarboranes: Synthesis, reactivity, and catalytic properties in alkene hydrogenation. *J. Am. Chem. Soc.* **2000**, *122*, 1963–1973. [[CrossRef](#)]
28. Teixidor, F.; Flores, M.A.; Viñas, C.; Kivekäs, R.; Sillanpää, R. [Rh(7-SPh-8-Me-7,8-C2B9H10)(PPh 3)2]: A new rhodacarborane with enhanced activity in the hydrogenation of 1-alkenes. *Angew. Chem. Int. Ed.* **1996**, *35*, 2251–2253. [[CrossRef](#)]
29. Mitani, M.; Saito, J.; Ishii, S.I.; Nakayama, Y.; Makio, H.; Matsukawa, N.; Matsui, S.; Mohri, J.I.; Furuyama, R.; Terao, H.; *et al.* FI catalysts: New olefin polymerization catalysts for the creation of value-added polymers. *Chem. Rev.* **2004**, *4*, 137–158. [[CrossRef](#)] [[PubMed](#)]
30. Martinez, A.; Hemmert, C.; Meunier, B. A macrocyclic chiral manganese(III) Schiff base complex as an efficient catalyst for the asymmetric epoxidation of olefins. *J. Catal.* **2005**, *234*, 250–255. [[CrossRef](#)]
31. Kruppa, M.; König, B. Reversible coordinative bonds in molecular recognition. *Chem. Rev.* **2006**, *106*, 3520–3560. [[CrossRef](#)] [[PubMed](#)]

32. Burzlaff, N. Tripodal N,N,O-ligands for metalloenzyme models and organometallics. *Adv. Inorg. Chem.* **2008**, *60*, 101–165.
33. Weber, B. Spin crossover complexes with N<sub>4</sub>O<sub>2</sub> coordination sphere—The influence of covalent linkers on cooperative interactions. *Coord. Chem. Rev.* **2009**, *253*, 2432–2449. [[CrossRef](#)]
34. Kuźnik, N.; Wyskocka, M. Iron(III) Contrast Agent Candidates for MRI: A Survey of the Structure-Effect Relationship in the Last 15 Years of Studies. *Eur. J. Inorg. Chem.* **2016**, *2016*, 445–458. [[CrossRef](#)]
35. Spokoiny, A.M. New Ligand platforms featuring boron-rich clusters as organomimetic substituents. *Pure Appl. Chem.* **2013**, *85*, 903–919. [[CrossRef](#)] [[PubMed](#)]
36. Viñas, C.; Teixidor, F.; Núñez, R. Boron clusters-based metallodendrimers. *Inorg. Chim. Acta* **2014**, *409*, 12–25. [[CrossRef](#)]
37. Timofeev, S.V.; Sivaev, I.B.; Prikaznova, E.A.; Bregadze, V.I. Transition metal complexes with charge-compensated dicarbollide ligands. *J. Organomet. Chem.* **2014**, *751*, 221–250. [[CrossRef](#)]
38. Farràs, P.; Juárez-Pérez, E.J.; Lepšík, M.; Luque, R.; Núñez, R.; Teixidor, F. Metallacarboranes and their interactions: Theoretical insights and their applicability. *Chem. Soc. Rev.* **2012**, *41*, 3445–3463. [[CrossRef](#)] [[PubMed](#)]
39. Štíbr, B. Reactions associated with arene replacement in bis-(arene) iron complexes. *J. Organomet. Chem.* **2012**, *716*, 1–5. [[CrossRef](#)]
40. Deng, L.; Xie, Z. Advances in the chemistry of carboranes and metallacarboranes with more than 12 vertices. *Coord. Chem. Rev.* **2007**, *251*, 2452–2476. [[CrossRef](#)]
41. Corsini, M.; de Biani, F.F.; Zanello, P. Mononuclear metallacarboranes of groups 6–10 metals: Analogues of metallocenes. Electrochemical and X-ray structural aspects. *Coord. Chem. Rev.* **2006**, *250*, 1351–1372. [[CrossRef](#)]
42. Nakamura, H.; Aoyagi, K.; Yamamoto, Y. Synthetic utility of *o*-carborane: Novel protective group for aldehydes and ketones. *J. Organomet. Chem.* **1999**, *574*, 107–115. [[CrossRef](#)]
43. Nakamura, H.; Aoyagi, K.; Yamamoto, Y. *o*-Carborane as a Novel Protective Group for Aldehydes and Ketones. *J. Org. Chem.* **1997**, *62*, 780–781. [[CrossRef](#)]
44. Terrasson, V.; Planas, J.G.; Prim, D.; Viñas, C.; Teixidor, F.; Light, M.E.; Hursthouse, M.B. Cooperative Effect of Carborane and Pyridine in the Reaction of Carboranyl Alcohols with Thionyl Chloride: Halogenation versus Oxidation. *J. Org. Chem.* **2008**, *73*, 9140–9143. [[CrossRef](#)] [[PubMed](#)]
45. Terrasson, V.; Giner Planas, J.; Prim, D.; Teixidor, F.; Viñas, C.; Light, M.E.; Hursthouse, M.B. General Access to Aminobenzyl-*o*-carboranes as a New Class of Carborane Derivatives: Entry to Enantiopure Carborane-Amine Combinations. *Chem. Eur. J.* **2009**, *15*, 12030–12042. [[CrossRef](#)] [[PubMed](#)]
46. Terrasson, V.; Garcia, Y.; Farras, P.; Teixidor, F.; Viñas, C.; Giner Planas, J.; Prim, D.; Light, M.E.; Hursthouse, M.B. Crystal engineering of *o*-carboranyl alcohols: Syntheses, crystal structures and thermal properties. *CrystEngComm* **2010**, *12*, 4109–4123. [[CrossRef](#)]
47. Terrasson, V.; Planas, J.G.; Viñas, C.; Teixidor, F.; Prim, D.; Light, M.E.; Hursthouse, M.B. *Closo-o*-Carboranylmethylamine-Pyridine Associations: Synthesis, Characterization, and First Complexation Studies. *Organometallics* **2010**, *29*, 4130–4134. [[CrossRef](#)]
48. Di Salvo, F.; Camargo, B.; Garcia, Y.; Teixidor, F.; Viñas, C.; Giner Planas, J.; Light, M.E.; Hursthouse, M.B. Supramolecular architectures in *o*-carboranyl alcohols bearing *N*-aromatic rings: Syntheses, crystal structures and melting points correlation. *Crystengcomm* **2011**, *13*, 5788–5806. [[CrossRef](#)]
49. Tsang, M.Y.; Di Salvo, F.; Teixidor, F.; Viñas, C.; Giner Planas, J.; Choquesillo-Lazarte, D.; Vanthuyne, N. Is Molecular Chirality Connected to Supramolecular Chirality? The Particular Case of Chiral 2-Pyridyl Alcohols. *Cryst. Growth Des.* **2015**, *15*, 935–945. [[CrossRef](#)]
50. Ching, H.Y.V.; Buck, D.P.; Bhadbhade, M.; Collins, J.G.; Rendina, L.M. A ternary supramolecular system containing a boronated DNA-metallointercalator, β-cyclodextrin and the hexanucleotide d(GTTCGAC) 2. *Chem. Commun.* **2012**, *48*, 880–882. [[CrossRef](#)] [[PubMed](#)]
51. Ching, H.Y.V.; Clifford, S.; Bhadbhade, M.; Clarke, R.J.; Rendina, L.M. Synthesis and supramolecular studies of chiral boronated platinum(ii) complexes: Insights into the molecular recognition of carboranes by β-cyclodextrin. *Chem. Eur. J.* **2012**, *18*, 14413–14425. [[CrossRef](#)] [[PubMed](#)]
52. Tsang, M.Y.; Viñas, C.; Teixidor, F.; Planas, J.G.; Conde, N.; SanMartin, R.; Herrero, M.T.; Dominguez, E.; Lledos, A.; Vidossich, P.; *et al.* Synthesis, Structure, and Catalytic Applications for ortho- and meta-Carboranyl Based NBN Pincer-Pd Complexes. *Inorg. Chem.* **2014**, *53*, 9284–9295. [[CrossRef](#)] [[PubMed](#)]

53. Di Salvo, F.; Paterakis, C.; Tsang, M.Y.; Garcia, Y.; Viñas, C.; Teixidor, F.; Giner Planas, J.; Light, M.E.; Hursthouse, M.B.; Choquesillo-Lazarte, D. Synthesis and Crystallographic Studies of Disubstituted Carboranyl Alcohol Derivatives: Prevailing Chiral Recognition? *Cryst. Growth Des.* **2013**, *13*, 1473–1484.
54. Di Salvo, F.; Tsang, M.Y.; Teixidor, F.; Viñas, C.; Planas, J.G.; Crassous, J.; Vanthuyne, N.; Aliaga-Alcalde, N.; Ruiz, E.; Coquerel, G.; *et al.* A Racemic and Enantiopure Unsymmetric Diiron(III) Complex with a Chiral *o*-Carborane-Based Pyridylalcohol Ligand: Combined Chiroptical, Magnetic, and Nonlinear Optical Properties. *Chem. Eur. J.* **2014**, *20*, 1081–1090. [[CrossRef](#)] [[PubMed](#)]
55. Tsang, M.Y.; Teixidor, F.; Viñas, C.; Choquesillo-Lazarte, D.; Aliaga-Alcalde, N.; Planas, J.G. Synthesis, Structures and Properties of iron(III) complexes with (*o*-carboranyl)bis-(2-hydroxymethyl)pyridine: Racemic *versus* meso. *Inorg. Chim. Acta* **2016**. [[CrossRef](#)]
56. Satapathy, R.; Dash, B.P.; Zheng, C.; Maguire, J.A.; Hosmane, N.S. Carboranypyrrroles: A Synthetic Investigation. *J. Org. Chem.* **2011**, *76*, 3562–3565. [[CrossRef](#)] [[PubMed](#)]
57. Yinghuai, Z.; Shiwei, X.; Vangala, V.R.; Chia, S.C.; Cheong, A.; Qin, O.N.; Hosmane, N.S. Carboranylimine-complexed titanium (IV) organometallics: An investigation of synthesis, structure and catalytic polymerization. *J. Organomet. Chem.* **2012**, *721–722*, 119–123. [[CrossRef](#)]
58. El-Zaria, M.E.; Arai, H.; Nakamura, H. *m*-Carborane-Based Chiral NBN Pincer-Metal Complexes: Synthesis, Structure, and Application in Asymmetric Catalysis. *Inorg. Chem.* **2011**, *50*, 4149–4161. [[CrossRef](#)] [[PubMed](#)]
59. Crassous, J. Chiral transfer in coordination complexes: Towards molecular materials. *Chem. Soc. Rev.* **2009**, *38*, 830–845. [[CrossRef](#)] [[PubMed](#)]
60. Di Salvo, F.; Teixidor, F.; Viñas, C.; Giner Planas, J.; Light, M.E.; Hursthouse, M.B.; Aliaga-Alcalde, N. Metallosupramolecular Chemistry of Novel Chiral *closo-o*-Carboranylalcohol Pyridine and Quinoline Ligands: Syntheses, Characterization, and Properties of Cobalt Complexes. *Cryst. Growth Des.* **2012**, *12*, 5720–5736. [[CrossRef](#)]
61. Ching, H.Y.V.; Clarke, R.J.; Rendina, L.M. Supramolecular  $\beta$ -Cyclodextrin Adducts of Boron-Rich DNA Metallointercalators Containing Dicarba-*closo*-dodecaborane(12). *Inorg. Chem.* **2013**, *52*, 10356–10367. [[CrossRef](#)] [[PubMed](#)]
62. Teixidor, F.; Benakki, R.; Viñas, C.; Kivekäs, R.; Sillanpää, R. Partial Degradation of the New *exo*-Heterodisubstituted Carborane Derivatives with d10 Transition Metal Ions (Cu, Au). *Inorg. Chem.* **1999**, *38*, 5916–5919. [[CrossRef](#)]
63. Viñas, C.; Mar Abad, M.; Teixidor, F.; Sillanpää, R.; Kivekäs, R. Reactions of Pd(II) with *closo*-1,2-dicarbadodecaborane-1,2-diphosphines. *J. Organomet. Chem.* **1998**, *555*, 17–23. [[CrossRef](#)]
64. Teixidor, F.; Viñas, C.; Abad, M.M.; Kivekäs, R.; Sillanpää, R. The formation of nido [7,8-(PR<sub>2</sub>)<sub>2</sub>-7,8-C<sub>2</sub>B<sub>9</sub>H<sub>10</sub>]<sup>−</sup> from *closo* 1,2-(PR<sub>2</sub>)<sub>2</sub>-1,2-C<sub>2</sub>B<sub>10</sub>H<sub>10</sub> (R = Ph, Et, *i*Pr or OEt): A process enhanced by complexation. *J. Organomet. Chem.* **1996**, *509*, 139–150. [[CrossRef](#)]
65. Teixidor, F.; Viñas, C.; Sillanpää, R.; Kivekäs, R.; Casabo, J. Nido-Carborane-Containing Compounds Resulting from the Reaction of *closo*-Carboranes with Transition Metal Complexes. *Inorg. Chem.* **1994**, *33*, 2645–2650. [[CrossRef](#)]
66. Teixidor, F.; Viñas, C.; Mar Abad, M.; Lopez, M.; Casabo, J. Synthesis of [7,8-(PPh<sub>2</sub>)<sub>2</sub>-7,8-C<sub>2</sub>B<sub>9</sub>H<sub>10</sub>]<sup>−</sup>: A ligand analogous to 1,2-bis(diphenylphosphino)ethane with a “built-in” negative charge. *Organometallics* **1993**, *12*, 3766–3768. [[CrossRef](#)]
67. Todd, J.A.; Rendina, L.M. The first examples of platinum(II)-amine complexes containing 1,2-dicarba-*closo*-dodecaborane(12). *Inorg. Chem. Commun.* **2004**, *7*, 289–291. [[CrossRef](#)]
68. Yoo, J.; Do, Y. Synthesis of stable platinum complexes containing carborane in a carrier group for potential BNCT agents. *Dalton Trans.* **2009**, 4978–4986. [[CrossRef](#)] [[PubMed](#)]
69. Suttill, J.A.; McGuinness, D.S.; Gardiner, M.G.; Evans, S.J. Ethylene polymerisation and oligomerisation with arene-substituted phenoxy-imine complexes of titanium: Investigation of multi-mechanism catalytic behaviour. *Dalton Trans.* **2013**, *42*, 4185–4196. [[CrossRef](#)] [[PubMed](#)]
70. Terao, H.; Ishii, S.; Mitani, M.; Tanaka, H.; Fujita, T. Ethylene/Polar Monomer Copolymerization Behavior of Bis(phenoxy-imine)Ti Complexes: Formation of Polar Monomer Copolymers. *J. Am. Chem. Soc.* **2008**, *130*, 17636–17637. [[CrossRef](#)] [[PubMed](#)]
71. Di Salvo, F.; Teixidor, F.; Viñas, C.; Giner Planas, J. A Distinct Tetradentate N<sub>2</sub>O<sub>2</sub>-type Ligand: (*o*-Carboranyl)bis(2-hydroxymethyl)pyridine. *Z. Anorg. Allg. Chem.* **2013**, *639*, 1194–1198. [[CrossRef](#)]

72. Knight, P.D.; Scott, P. Predetermination of chirality at octahedral centres with tetradentate ligands: Prospects for enantioselective catalysis. *Coord. Chem. Rev.* **2003**, *242*, 125–143. [[CrossRef](#)]
73. Knof, U.; von Zelewsky, A. Predetermined Chirality at Metal Centers. *Angew. Chem. Int. Ed.* **1999**, *38*, 302–322. [[CrossRef](#)]
74. Vigato, P.A.; Peruzzo, V.; Tamburini, S. Acyclic and cyclic compartmental ligands: Recent results and perspectives. *Coord. Chem. Rev.* **2012**, *256*, 953–1114. [[CrossRef](#)]
75. Kanazawa, Y.; Tsuchiya, Y.; Kobayashi, K.; Shiomi, T.; Itoh, J.-I.; Kikuchi, M.; Yamamoto, Y.; Nishiyama, H. Asymmetric Conjugate Reduction of  $\alpha,\beta$ -Unsaturated Ketones and Esters with Chiral Rhodium(2,6-bisoxazolinyphenyl) Catalysts. *Chem. Eur. J.* **2006**, *12*, 63–71. [[CrossRef](#)] [[PubMed](#)]
76. Nishiyama, H. Synthesis and use of bisoxazoliny-phenyl pincers. *Chem. Soc. Rev.* **2007**, *36*, 1133–1141. [[CrossRef](#)] [[PubMed](#)]



© 2016 by the authors; licensee MDPI, Basel, Switzerland. This article is an open access article distributed under the terms and conditions of the Creative Commons Attribution (CC-BY) license (<http://creativecommons.org/licenses/by/4.0/>).